Criticality Characterization of Plutonium – Iron Systems

Arielle Miller,[a] Jerry McKamy[b]

[a]2725 39th St NW Apt 209, Washington, DC 20007, millerarielle15@gmail.com
[b]12501 Copen Meadow Ct, Gaithersburg, MD 20878, jnmisbatman1@yahoo.com

INTRODUCTION

The purpose of this work is sensitivity analyses for plutonium-239 solutions containing iron bearing solids as a suspension and suggest guidance for a path forward towards setting defensible upper subcritical limits. Such a system has relevance to plutonium processing residue storage. To do this, we first characterize a plutonium nitrate solution with varying concentrations of iron to determine if the current suite of benchmarks in the International Criticality Safety Benchmark Experiment Project (ICSBEP) [1] are applicable. Concentrations of iron include amounts that drive the system subcritical (e.g., analog to waste systems using high concentrations of impurities to control criticality). Applicable benchmarks exist for the application of iron concentration in plutonium nitrate solutions up to an iron-to-plutonium-239 (Fe/Pu) ratio of 0.2 g/g. For iron concentrations above this ratio (where the system cannot be driven critical) there does not exist any applicable benchmarks and we propose a path forward for addressing this data gap.

CALCULATIONAL WORK

A plutonium nitrate solution (^{239}Pu only isotope modeled) was modeled in SCALE6.2.1 (KENOVI) as a sphere for a range of moderation ratios (H/Pu) at room temperature (27C). The range of nitric acid molarity was chosen to be 0.5 to 6 M. The plutonium nitrate sphere was modeled with 30 cm of water reflection. The Pu concentration (g/L) were calculated using the ARH-600 method [2]. The embedded Pitzer Method [3] in SCALE was utilized to calculate the density of the $Pu(NO_3)_4$ solution for each H/Pu and M_{HNO3} pair. This pure plutonium nitrate sphere was used to determine the critical mass and radius for the various H/Pu and M_{HNO3} pairs. Figure 1 provides a graph of critical plutonium mass versus density for 0.5 M and 6.0 M nitric acid and the Pu-Water bounding case.

Using the critical mass and radius of a chosen H/Pu = 1100 and M_{HNO3} = 6.0 M, iron was introduced to the model. Iron-to-plutonium (Fe/Pu) ratios were applied to determine the applicable amount of ^{56}Fe to add to the $Pu(NO_3)_4$ system. Fe/Pu (g/g) from 0.001 to 10 were evaluated. Critical radius of the $Pu(NO_3)_4$ system (1100, 6M) was recalculated for the various Fe/Pu ratios. It was determined that criticality could not be achieved for a $Pu(NO_3)_4$ system with a Fe/Pu ratio greater than 0.2 g/g (Figure 2).

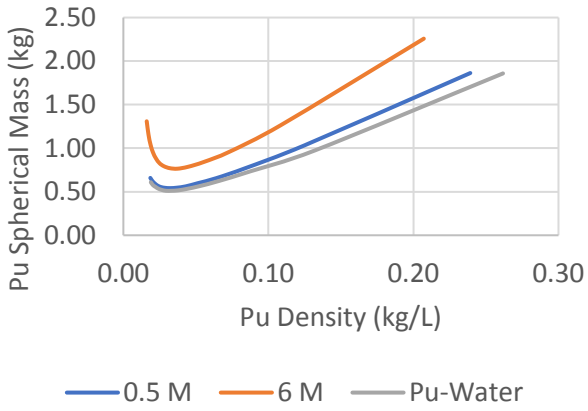

Fig. 1. Critical Masses of Homogenous Plutonium Spheres.

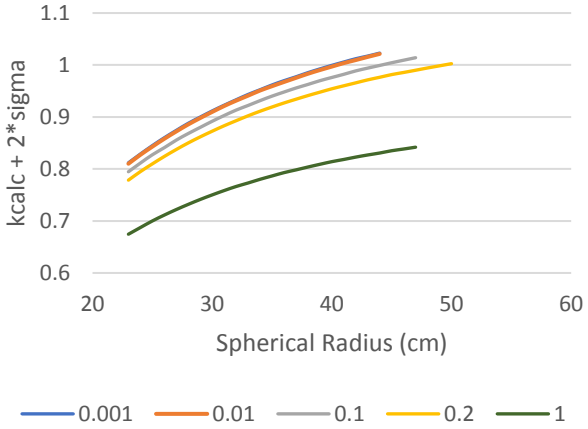

Fig. 2. k_{eff} for Plutonium Nitrate Solutions at Various Fe/Pu Concentrations.

RESULTS

Sensitivity profiles were generated using TSUNAMI-1D for the $Pu(NO_3)_4$ system with the various Fe/Pu ratios. Sensitivity profiles were also generated for 135 benchmark systems from Volume I of the ICSBEP [1]. All benchmarks were plutonium solutions in a thermal energy (PU-SOL-THERM). Neutron production ($\upsilon\Sigma_f\varphi$) (normalized by lethargy) was generated to compare the neutron production (per lethargy) versus energy (log-log plot). These plots were generated for both the $Pu(NO_3)_4$ system with the various Fe/Pu ratios and the benchmark experiments. The neutron

production spectra were compared, and it was determined that most of the benchmark experiments were a good fit with the $Pu(NO_3)_4$ system with Fe/Pu ratios 0.001, 0.01, 0.01 – 1. For Fe/Pu = 1 and 10 g/g the neutron production spectra begins to diverge from the benchmark experiments in the thermal region. For some other benchmarks (PU-SOL-THERM-013 through 017 [1]) there was no correlation in the neutron production spectra regardless of energy regime or Fe/Pu ratio. This lack of neutron production correlation between benchmarks PU-SOL-THERM-013 through 017 [1] is coupled with low sensitivities in ^{56}Fe (n,γ) regardless of ^{56}Fe concentration for these benchmarks.

Figure 3 provides the plot of neutron production versus energy of the calculation model at various Fe/Pu ratios to the benchmark experiment case. It illustrates that despite the large differences in iron concentrations (as shown in Table I) there is relatively good correlation between the low Fe/Pu ratios and the Pu benchmark experiment cases similar to PU-SOL-THERM-005-003 [1] over the entire energy spectrum. Most importantly in the thermal range around the 10^{-2} eV range. The Fe/Pu = 10 g/g curve (orange) begins to show a visible separation between the benchmark at the thermal energy range. The fission neutron production is low in the thermal range due to the increased absorption of Fe^{56} via n,γ reactions as the concentration of ^{56}Fe has increased.

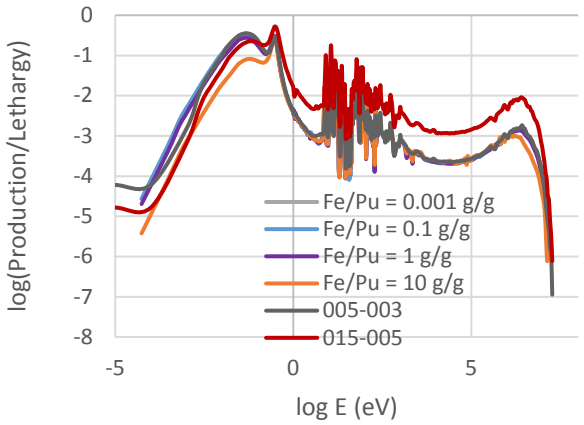

Fig. 3. Neutron Production v. Energy (log-log scale) for Iron Calculation Models.

TABLE I. ^{56}Fe Concentrations for Calculations Models	
Fe/Pu (g/g)	N_{Fe} (at-b/cm)
0.001	1.23213E-05
0.01	0.000123213
0.1	0.00123213
1	0.0123213
10	0.123213

Figure 3 also illustrates that PU-SOL-THERM-015-005 [1] (red) is not well fit to any of the calculational models over any of the energies. PU-SOL-THERM-015-005 [1] has more ^{56}Fe than PU-SOL-THERM-005-003 [1] (olive green). So its lower fission neutron production in the thermal range could be attributed to an increase in n,γ reactions from ^{56}Fe at that energy range. If that were true, the corresponding sensitivity plots for these two benchmark cases would show a proportionality between sensitivity for n,γ reactions for ^{56}Fe and concentration of ^{56}Fe. However, as shown in Figure 4, the opposite is present. If, the entire fission neutron spectrum for PU-SOL-THERM-0015-005 [1] (and the family of benchmarks PU-SOL-THERM-013 through 016 [1]) is examined from Figure 3, it becomes evident that the spectrum is hardened in comparison to PU-SOL-THERM-005-003 [1] (and its family of benchmarks 1 through 12).

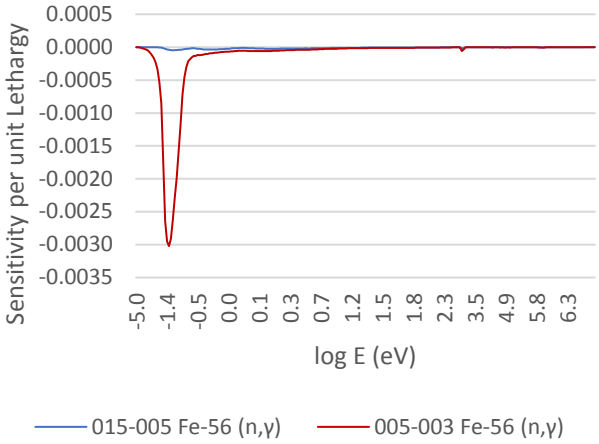

Fig. 4. ^{56}Fe Sensitivities for n,γ Reactions in 015-005 (blue) and 005-003 (red) from ENDF/B-VII.0 238 Group [5].

Figure 5 compares the two dominant cross sections in the thermal and epithermal regions, elastic collisions and n,γ reactions. The n,γ reaction, which supports neutron absorptions, dominates narrowly at very low energies. Elastic collisions dominate into the epithermal range with a narrow window for n,γ dominance at around 1 keV. The resonances for elastic and n,γ overlap at the high keV range competing with n,n' and inelastic scattering. At high energies in the fast region n,γ is no longer relevant.

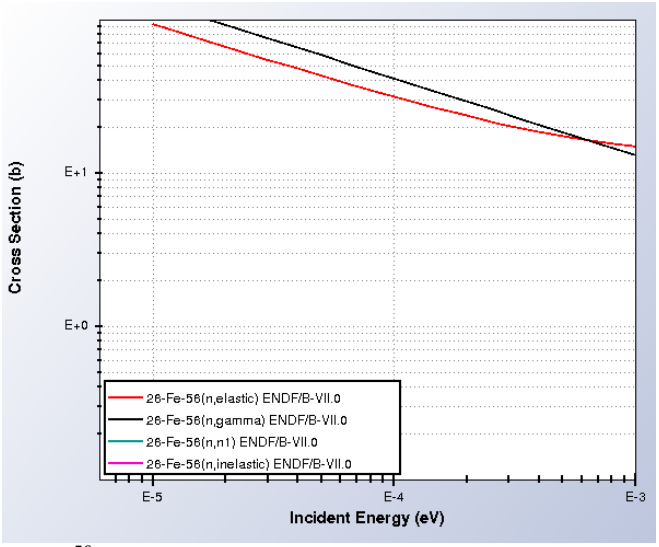

Fig. 5. ^{56}Fe Cross Sections for Major Reaction Channels [4].

Focusing in further on the $1e^{-6}$ to $1e^{-3}$ eV range there is a transition point where elastic collisions dominate over n,γ reactions at around $1e^{-3}$ eV. This coincides with the fission spectrum of benchmark 015-005 versus 005-003. Since the neutron spectrum in benchmark 015-005 is harder there are less thermal neutrons. One effect is a lower fission neutron production within the thermal energy range. The other effect that is seen in a transition from n,γ reactions (black) in ^{56}Fe to elastic collisions (red) between ^{56}Fe and neutrons. Figures 6a and 6b, sensitivity plots of Fe^{56} reaction channels illustrates this point (red = n,γ reactions and blue = elastic collisions). This is why even though, there is more ^{56}Fe physically in the 015-005 benchmark than in the 005-003 benchmark, the sensitivity to ^{56}Fe n,γ reactions is greater in latter than the former (Figure 4).

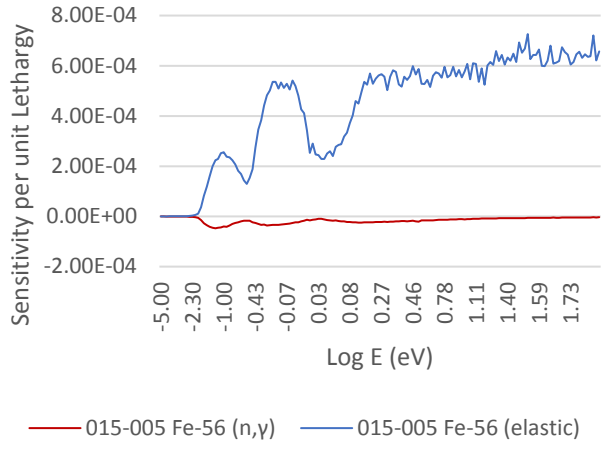

Fig. 6(a). ^{56}Fe Sensitivities for Major Reaction Channels in 015-005 [5].

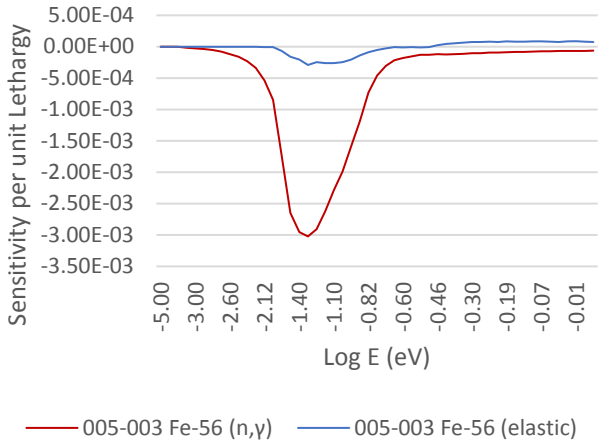

Fig. 6(b). ^{56}Fe Sensitivities for Major Reaction Channels in 005-003 [5].

Figure 7 provides the sensitivity profiles for the $Pu(NO_3)_4$ system with the various Fe/Pu ratios. It indicates an increasing sensitivity of ^{56}Fe corresponding to an increase in ^{56}Fe concentration for Fe/Pu = 0.001 – 10 g/g.

TABLE II. Sensitivity of ^{56}Fe for Various Fe/Pu Ratios

Fe/Pu (g/g)	TSUNAMI-1D (n,γ)	TSUNAMI-1D (total)	Direct Perturbation (total)
0.001	-0.0272%	-0.0239%	
0.01	-0.2711%	-0.2389%	
0.1	-2.634%	-2.347%	-2.346%
1	-20.134%	-18.003%	-17.982%
10	-57.738%	-54.297%	-54.265%

Table II provides the sensitivity values that correspond to the Fe/Pu ratios from Figure 7.

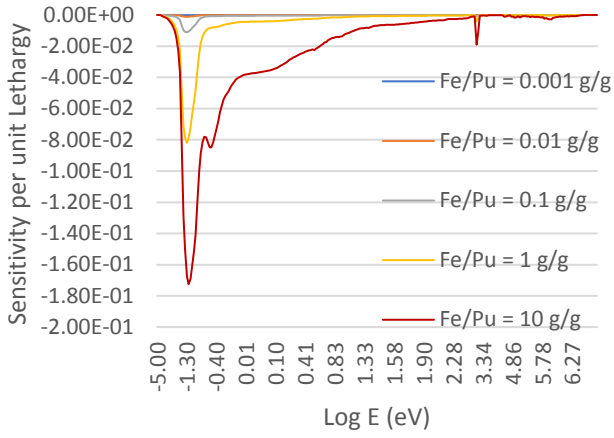

Fig. 7. Sensitivity Profiles for ^{56}Fe for Plutonium Nitrate Solution.

The sensitivity profiles of the $Pu(NO_3)_4$ system with the various Fe/Pu ratios were compared to the sensitivity profiles of the 135 benchmark experiments using TSUNAMI-IP. A c_k and E_{sum} greater than 0.8 and an "g-value" of greater than 0.9 for nuclide-reaction for ^{56}Fe [6,7]. This comparison was performed to determine the number of applicable benchmarks for the $Pu(NO_3)_4$ system with the various Fe/Pu ratios (13 applications). Table III lists the results of this comparison produced applicable benchmarks for Fe/Pu = 0.001, 0.01, 0.1, 0.2, 1, and 10 g/g. When comparing the variance in the data uncertainties (c_k) there are no applicable benchmarks that are within 80% of the variance when Fe/Pu is greater than 0.2 g/g. When comparing the sensitivity of k_{eff} to its constituent cross-section data common between the application and the experiment (E_{sum}) there are no applicable benchmarks within 80% of the sensitivity when Fe/Pu is greater than 9 g/g. Comparing the "g-value" for the energy-dependent sensitivity of k_{eff} the ^{56}Fe nuclide-reaction pair for n,γ reactions between the experiment and the application there are no applicable benchmarks when Fe/Pu is greater than 0.1 g/g.

TABLE III. Sensitivity of ^{56}Fe for Various Fe/Pu Ratios

Criterion	Fe/Pu Ratio (g/g)					
	0.001	0.01	0.1	0.2	1	10
$c_k > 0.8$	64	64	58	39	0	0
$E_{sum} > 0.8$	132					0
g > 0.9-^{56}Fe n,γ	69	48	0	0	0	0
g > 0.9-^{56}Fe total	49	48	0	0	0	0

CONCLUSION

There are applicable benchmarks for the systems utilizing iron in low enough concentrations that criticality is still possible (Fe/Pu ≤ 0.2 g/g). It is imperative to understand the dominant reaction channels in a specific benchmark and ensure they match with those in the application model. It would be potentially problematic to simply assume a benchmark is applicable because it has similar nuclides to the application in question.

For applications of plutonium nitrate solutions where iron is included in the fissile solution in concentrations high enough to drive the system subcritical, there are not subcritical benchmarks. This appears to occur around Fe/Pu > 0.2 g/g. For systems which are crediting iron as a neutron absorber for the purpose of criticality control, it is recommended that a USL of 0.8 be utilized due to the lack of applicable benchmarks [8]. An USL this low should not inhibit effective operations due to the expected large margin of subcriticality provided by the iron in the actual system. As we have shown, any system with a Fe/Pu ratio > 0.2 g/g will be subcritical. The larger the Fe/Pu ratio the larger the margin of subcriticality of the system.

In lieu of selecting a USL of 0.8, it is recommended that a suite of subcritical experiments benchmarking the application of concern be conducted [8]. Finally, if other parameters (e.g., geometry, mass, etc…) can be credited instead of the neutron absorber iron, it is recommended that one of those parameters be credited as a neutron control.

ACKNOWLEDGMENTS

The views expressed herein are solely those of the authors, and no official support or endorsement by any organization or group including but not limited to that of the authors' employers or the U.S. Government is intended or should be inferred.

REFERENCES

1. International Handbook of Evaluated Criticality Safety Benchmark Experiments, NEA/NSC/DOC(95)/03, OECD-NEA, Paris, France (2017).
2. R. CARTER, "Criticality Handbook," ARH-600 Handbook – Volume II, Richland, WA (1969).
3. C. HOPPER, "Application of the Pitzer Method for Modeling Densities of Actinide Solutions in the SCALE Code System," **153**, *Nuclear Technology* (2006).
4. Evaluated Nuclear Data File (ENDF) Retrieval & Plotting (Sigma), ENDF/B-VII.0, https://www.nndc.bnl.gov/sigma/.
5. Database for the International Criticality Safety Benchmark Evaluation Project, NEA/NSC/DOC(95)03/II, OECD-NEA, Paris, France (2017).
6. B. BROADHEAD, "Sensitivity- and Uncertainty-Based Criticality Safety Validation Techniques," *Nuclear Science and Engineering*, **146**, 340-366 (2004).
7. B. REARDEN, "SCALE 6.2 Manual," ORNL/TM-2005/39, Oak Ridge, TN (2016).
8. Criticality Safety Support Group, "Validation with Limited Benchmarks," Response to Tasking 2014-02 (2015).